6th European Conference on Computational Mechanics (ECCM 6)
7th European Conference on Computational Fluid Dynamics (ECFD 7)
1115 June 2018, Glasgow, UK

UNCERTAINTY QUANTIFICATION AND ROBUST DESIGN FOR AERODYNAMIC APPLICATIONS, USING CONTINUOUS ADJOINT METHODS

Anastasios K. Papageorgiou[1], Kimon B. Fragkos[1], Evangelos M. Papoutsis-Kiachagias[1] and Kyriakos C. Giannakoglou[1]

[1] National Technical University of Athens (NTUA), School of Mechanical Engineering, Parallel CFD & Optimization Unit, Athens, Greece,
e-mail: vaggelisp@gmail.com, kimonfragos@gmail.com, tkpapageorgiou@gmail.com, kgianna@central.ntua.gr

Key words: *Uncertainty Quantification, Robust Design, Method of Moments, Intrusive Polynomial Chaos Expansion, Continuous Adjoint Methods*

Abstract. In CFD-based applications, propagating uncertainties associated with the operating conditions or shape imperfections from the system input to its output, a.k.a. uncertainty quantification (UQ), and optimization under uncertainties (robust design) are at the cutting edge of research. In gradient-based robust design, the computation of the gradient of an objective function which accounts for all uncertainties is required. In this paper, two UQ methods are developed and presented; the first one is based on the Method of Moments (MoM, [7]) and the second on the intrusive Polynomial Chaos Expansion (iPCE), both for incompressible fluid flows. Regarding optimization, a combination of the mean value and standard deviation of a quantity of interest (QoI, for instance drag or lift) forms the objective function to be minimized; in this paper, continuous adjoint-enabled, gradient-based methods will be used to minimize it. The adjoint to both UQ methods is presented. The iPCE-based method requires the development and validation of the adjoint to the iPCE PDEs. With the MoM and, in particular, its first-order variant, the objective function includes the first derivatives of the QoI with respect to (w.r.t.) the uncertain variables which are then differentiated w.r.t. the design variables to minimize it. To avoid costly computations, this paper proposes the computation of projections of the second-order b-c mixed derivatives to vectors, instead of the Hessian matrix itself. A combination of the continuous adjoint and direct differentiation can efficiently compute this projection, leading to an overall cost per optimization cycle that is independent from the number of both the uncertain and the design variables. The flow problem around an isolated airfoil is studied with all methods; the validation of the computed derivatives is presented.

1 Introduction

Most shape optimization techniques consider all inputs known with absolute certainty. As a result, the solution optimality refers exclusively to a single operating point. However, in real problems, the environmental conditions may vary within a certain range. These varying conditions are usually referred to as uncertain variables and follow a certain statistical distribution (normal, Weibull etc.) which is either known or assumed to be known and expressed through their mean values and standard deviations. Therefore, there is a need to develop UQ tools in order to propagate the flow uncertainties from the system input to its output; the latter is, herein, referred to as the QoI and is, practically, the one that would have been optimized in case uncertainties were ignored. In case the target is to optimize an aerodynamic shape, by also considering uncertainties, the new objective function should be expressed in terms of the mean value and standard deviation of the QoI. Usually, combining the first two statistical moments of the QoI is enough. In case a gradient-based optimization method is to be used, the gradient of this objective function w.r.t. the design variables should be computed, too.

Some methods that are often used to propagate uncertainties are the Monte-Carlo (MC) or Quasi-MC, MoM and PCE ones ([**?**],[7],[1]). The latter appears in two variants, namely the intrusive and the non-intrusive one. All methods based on Monte-Carlo techniques are straightforward and demand a considerably high number of CFD evaluations which make them unaffordable. This paper presents the mathematical formulation and assessment of iPCE and MoM, both of which have a significantly lower computational cost than MC. The computed mean values and standard deviations are firstly validated with Monte-Carlo, which is used only as a reference. The next step is to proceed to the optimization of an objective function built by concatenating the mean value and standard deviation of the QoI. The optimization runs are done using gradient-based methods supported by continuous adjoint. Although PCE is frequently used during the last years ([4], [1], [2]), the adjoint to the iPCE PDEs for laminar, incompressible flows is presented for the first time in the literature. The advantage of iPCE compared to the non-intrusive approach is that the former is more accurate ([8]); hence, a lower chaos order can be used to obtain the same level of accuracy, eventually leading to a lower cost. Regarding the optimization with the first-order variant of the MoM, an idea borrowed from truncated Newton methods is used to avoid the computation of second-order derivatives; instead, their projections to certain vectors are computed at a much lower CPU cost. This optimization method will be referred to as the projected First Order-Second Moment (pFOSM) one.

2 Primal Equations, QoI and Objective Function

The governing equations are the steady state Navier-Stokes ones, for 2D laminar flows of an incompressible fluid

$$R^p = -\frac{\partial v_j}{\partial x_j} = 0 \tag{1a}$$

$$R_i^v = v_j \frac{\partial v_i}{\partial x_j} - \frac{\partial \tau_{ij}}{\partial x_j} + \frac{\partial p}{\partial x_i} = 0, \quad i = 1, 2 \tag{1b}$$

where v_i are the velocity components, $\tau_{ij} = \nu \left(\frac{\partial v_i}{\partial x_j} + \frac{\partial v_j}{\partial x_i} \right)$ the stress tensor components, p the static pressure divided by the fluid density and ν the kinematic viscosity of the fluid.

Without loss in generality, the drag force

$$F = \int_{S_w} (p\delta_i^j - \tau_{ij}) n_j r_i dS \tag{2}$$

is the QoI throughout this paper, where r_i is the farfield velocity direction. The objective function, to be minimized, for the optimization under uncertainties is the linear combination of the mean value (μ_F) and standard deviation (σ_F) of the QoI

$$J = w_0 \mu_F + w_1 \sigma_F \tag{3}$$

where w_0, w_1 are appropriate weights.

3 Uncertainty Quantification (UQ)

3.1 Method of Moments (MoM)

According to the method of statistical moments, the mean value and standard deviation of the QoI w.r.t. the uncertain variables $c_i, i \in [1, M]$, can be written, by taking into account only the first-order Taylor expansion term (First-Order Second-Moment, FOSM) ([7]), as,

$$\mu_F(c) = F|_{\bar{c}}, \qquad \sigma_F(c) = \sqrt{\left[\frac{\delta F}{\delta c_\mu} \right]_{\bar{c}}^2 \sigma_\mu^2} \tag{4}$$

From eq. 4, it can be seen that in FOSM, the mean value of the QoI is not taking into consideration the standard deviation of $\vec{c}$ and is computed at its mean value; this is not true, however, for the standard deviation of the QoI. The computation of J requires, apart from the flow field, the first-order derivatives of the QoI w.r.t. the uncertain variables, which are, herein, computed using the continuous adjoint method. Following the methodology presented in [6], the adjoint equations read

$$R^q = -\frac{\partial u_j}{\partial x_j} = 0 \tag{5a}$$

$$R_i^u = u_j \frac{\partial v_j}{\partial x_i} - \frac{\partial (v_j u_i)}{\partial x_j} - \frac{\partial \tau_{ij}^a}{\partial x_j} + \frac{\partial q}{\partial x_i} = 0, \quad i = 1, 2 \tag{5b}$$

where u_i are the adjoint velocity components, q the adjoint pressure and τ_{ij}^a the adjoint stress tensor. The adjoint boundary conditions are omitted in the interest of space.

In this paper, uncertainties are associated with the flow conditions and, in specific, the only uncertain variable is the free-stream flow angle a_∞, which is considered enough for demonstrating the proposed methods. So, after satisfying the adjoint PDEs and their boundary conditions, the gradient of F w.r.t. c_μ is computed through an integral along the inlet to the flow domain as follows

$$\frac{\delta F}{\delta c_\mu} = \int_{S_I} \left[\nu \left(\frac{\partial u_i}{\partial x_j} + \frac{\partial u_j}{\partial x_i} \right) n_j - q n_i \right] \frac{\delta v_i}{\delta c_\mu} dS \tag{6}$$

The $\delta v_i/\delta c_\mu$ term is, thus, computed analytically. It is assumed that the solution of the adjoint equations costs as much as the one of the primal equations. Each of the primal and adjoint fields is computed at the cost of one Equivalent Flow Solution (EFS), where EFS is the most appropriate time unit when comparing methods. Thus, with the FOSM approach, the computational cost for UQ is 2 Equivalent Flow Solutions (EFS).

3.2 The iPCE Method

According to the PCE method, each uncertain flow variable (e.g. pressure, velocity) is expressed as the sum of the products of deterministic coefficient fields $p_l(\vec{x})$ and orthogonal polynomials $H_l(\vec{\xi})$. For example, for the pressure p,

$$p(\vec{x},\vec{\xi}) = \sum_{l=0}^{L-1} p_l(\vec{x}) H_l(\vec{\xi}) \tag{7}$$

where $\vec{\xi}$ is the vector of uncertain variables. The total number of terms (L) depends on the number of the uncertain variables (M) and the chaos order (γ) and is equal to $L = \frac{(M+\gamma)!}{M!\gamma!}$. The higher the chaos order, the more accurate the UQ, at the expense though of a higher computational cost. In this paper, a normal distribution is assumed for each uncertain variable and, this is why, H_l stands for the Hermite polynomials.

In intrusive PCE, the expansions of the (uncertain) flow fields (eq. 7) are introduced to the governing equations; therefore, new PDEs are derived through Galerkin projections. The Galerkin projection of any orthogonal polynomial is defined as $\langle H_i, H_j\rangle = \int H_i(\vec{\xi}) H_j(\vec{\xi}) w(\vec{\xi}) d\vec{\xi}$, where $w(\vec{\xi})$ is the product of the probability density functions (PDF) of the normal distribution for each independent uncertain variable (ξ). By making use of the properties of Galerkin projections, L systems of PDEs similar to the Navier-Stokes ones are derived; the cost for solving them is $\approx L$ EFS. The new set of PDEs is

$${}^{l}R^{p} = -\frac{\partial v_{im}}{\partial x_i}\langle H_m, H_l\rangle = 0 \tag{8a}$$

$${}^{l}R^{v}_{i} = v_{jm}\frac{\partial v_{is}}{\partial x_j}\langle H_m, H_s, H_l\rangle + \frac{\partial p_m}{\partial x_i}\langle H_m, H_l\rangle - \frac{\partial}{\partial x_j}\left[\nu\left(\frac{\partial v_{jm}}{\partial x_i} + \frac{\partial v_{im}}{\partial x_j}\right)\right]\langle H_m, H_l\rangle = 0 \tag{8b}$$

For instance for, $M=1$ and $\gamma=2$, eqs. 8 give rise to 9 PDEs, for 2D incompressible flows, as follows

$$\begin{aligned}
&{}^{l}R^{p} = -\frac{\partial v_{il}}{\partial x_i} = 0, \quad l = 0,1,2\\
&{}^{0}R^{v}_{i} = v_{j0}\frac{\partial v_{i0}}{\partial x_j} + v_{j1}\frac{\partial v_{i1}}{\partial x_j} + 2v_{j2}\frac{\partial v_{i2}}{\partial x_j} + \frac{\partial p_0}{\partial x_i} - \frac{\partial}{\partial x_j}\left[\nu\left(\frac{\partial v_{j0}}{\partial x_i} + \frac{\partial v_{i0}}{\partial x_j}\right)\right] = 0\\
&{}^{1}R^{v}_{i} = v_{j1}\frac{\partial v_{i0}}{\partial x_j} + v_{j0}\frac{\partial v_{i1}}{\partial x_j} + 2v_{j1}\frac{\partial v_{i2}}{\partial x_j} + 2v_{j2}\frac{\partial v_{i1}}{\partial x_j} + \frac{\partial p_1}{\partial x_i} - \frac{\partial}{\partial x_j}\left[\nu\left(\frac{\partial v_{j1}}{\partial x_i} + \frac{\partial v_{i1}}{\partial x_j}\right)\right] = 0\\
&{}^{2}R^{v}_{i} = 4v_{j2}\frac{\partial v_{i2}}{\partial x_j} + v_{j1}\frac{\partial v_{i1}}{\partial x_j} + v_{j2}\frac{\partial v_{i0}}{\partial x_j} + v_{j0}\frac{\partial v_{i2}}{\partial x_j} + \frac{\partial p_2}{\partial x_i} - \frac{\partial}{\partial x_j}\left[\nu\left(\frac{\partial v_{j2}}{\partial x_i} + \frac{\partial v_{i2}}{\partial x_j}\right)\right] = 0
\end{aligned} \tag{9}$$

The expansions of the uncertain flow variables are introduced into the QoI in order to compute the deterministic coefficients of the QoI. These are

$$F_l = \int_S \Bigg(-\nu \Bigg(\frac{\partial v_{il}}{\partial x_j} + \frac{\partial v_{jl}}{\partial x_i} \Bigg) n_j + p_l n_i \Bigg) r_i dS \tag{10}$$

These coefficients are necessary in order to compute the mean value and standard deviation of the QoI, which are

$$\mu_F = F_0, \qquad \sigma_F = \sqrt{\sum_{l=0}^{L-1} F_i \langle H_i, H_l \rangle} \tag{11}$$

For $M = 1$ and $\gamma = 2$, $\sigma_F = \sqrt{F_1^2 + 2F_2^2}$. Once eqs. 8 have been solved, these integrals can be computed at a negligible CPU cost. The cost of solving eqs. 8 and, hence, of computing the mean value and the standard deviation is L EFS.

3.3 Assessment of the MoM and iPCE Methods

As already mentioned, the case examined is an isolated airfoil exanined in laminar, incompressible flow conditions. The uncertainty is introduced by the farfield flow angle, which has a mean value $\alpha_\infty = 4^o$ and a standard deviation $\sigma_{\alpha_\infty} = 0.3^o$. The Reynolds number of the flow is $Re = 3000$. In order to validate the UQ results, 3000 CFD evaluations were first performed with the Monte-Carlo method. The mean value and standard deviation computed by the expensive MC method are considered as reference values. Consequently, the statistical moments computed with FOSM and iPCE are compared with these reference values in table 1. Both methods estimate μ_F and σ_F without significant error (less than 0.01% for μ_F and 0.1% for σ_F).

Table 1: Comparison of the mean value and standard deviation of the QoI (drag) computed using MC, FOSM, iPCE.

	MC	FOSM	iPCE
μ_F	0.034999	0.035030	0.035003
$\sigma_F(10^{-4})$	1.5401	1.5507	1.5340

4 Gradient Computation and Optimization

4.1 Method of Moments (MoM)

A gradient-based shape optimization procedure requires the computation of $\frac{\delta J}{\delta b_n}$, where b_n ($n \in [1, N]$) are the design variables. The differentiation of eq. (3) gives

$$\frac{\delta J}{\delta b_n} = w_0 \frac{\delta F}{\delta b_n} + w_1 \frac{\sum_{\mu=1}^{M} \frac{\delta F}{\delta c_\mu} \frac{\delta^2 F}{\delta c_\mu \delta b_n} \sigma_\mu^2}{\sqrt{\sum_{\mu=1}^{M} \left[\frac{\delta F}{\delta c_\mu}\right]^2 \sigma_\mu^2}} \tag{12}$$

In order to compute the sensitivity derivatives of the objective function w.r.t. the design variables, it is necessary to compute three different groups of derivatives, specifically

$$\frac{\delta F}{\delta b_n}, \quad \left[\frac{\delta F}{\delta c_\mu}\right]^2 \sigma_\mu^2, \quad \sum_{\mu=1}^{M} \frac{\delta^2 F}{\delta c_\mu \delta b_n} \frac{\delta F}{\delta c_\mu} \sigma_\mu^2$$

The first-order derivatives can be computed from the solution of the continuous adjoint equations, section 3.1. The third term includes the second order derivatives $\frac{\delta^2 F}{\delta c_\mu \delta b_n}$, which will hereafter be referred to as mixed $b-c$ derivatives, multiplied by the vector $z_\mu = \{\frac{\delta F}{\delta c_\mu} \sigma_\mu^2\}$; the curly brackets indicate no summation over repeated indices. Hence,

$$\frac{\delta J}{\delta b_n} = w_0 \frac{\delta F}{\delta b_n} + w_1 \frac{\sum_{\mu=1}^{M} \frac{\delta^2 F}{\delta c_\mu \delta b_n} z_\mu}{\sqrt{\sum_{\mu=1}^{M} \left[\frac{\delta F}{\delta c_\mu}\right]^2 \sigma_\mu^2}} = w_0 \frac{\delta F}{\delta b_n} + w_1 \frac{\frac{\delta^2 F}{\delta c_\mu \delta b_n} z_\mu}{\sqrt{\left[\frac{\delta F}{\delta c_\mu}\right]^2 \sigma_\mu^2}} \tag{13}$$

The concept of pFOSM is inspired from the truncated Newton technique presented in [5]. Instead of separately computing the components of $\frac{\delta^2 F}{\delta c_\mu \delta b_n}$ and performing the contraction with z_μ, the method proposes to directly compute the projection of the $b-c$ mixed derivatives onto $\vec{z}$.

After satisfying eqs. (5), apart from computing $\frac{\delta F}{\delta c_\mu}$, $\frac{\delta F}{\delta b_n}$ can be expressed as, [3],

$$\begin{aligned} \frac{\delta F}{\delta b_n} = & \int_\Omega \left(q \frac{\partial v_j}{\partial x_k} - u_i v_j \frac{\partial v_i}{\partial x_k} - \tau_{ij}^a \frac{\partial v_i}{\partial x_k} + u_i \frac{\partial \tau_{ij}}{\partial x_k} - u_j \frac{\partial p}{\partial x_k} \right) \frac{\partial}{\partial x_j} \left(\frac{\delta x_k}{\delta b_n} \right) d\Omega \\ & + \int_{S_w} \left(p \delta_i^j - \tau_{ij} \right) r_i \frac{\delta \left(n_j dS \right)}{\delta b_n} = \int_\Omega A_{jk} \frac{\partial}{\partial x_j} \left(\frac{\delta x_k}{\delta b_n} \right) d\Omega + \int_{S_w} \left(p \delta_i^j - \tau_{ij} \right) r_i \frac{\delta \left(n_j dS \right)}{\delta b_n} \end{aligned} \tag{14}$$

Computing $\frac{\delta^2 F}{\delta c_\mu \delta b_n}$ by using a combination of adjoint and direct differentiation would result to a cost that scales with M, [7]. Instead, eq. 14 is differentiated w.r.t. c_μ and the result is projected to $\vec{z}$. Hence, only the projected derivatives of the primal and adjoint variables (e.g. $\tilde{v_i} = \frac{\delta v_i}{\delta c_\mu} z_\mu$) have to be computed, instead of the M fields (e.g. $\frac{\delta v_i}{\delta c_\mu}, \mu \in [1, M]$) that would have to be computed otherwise. The projected fields can be computed by

differentiating eqs.1 and 5 w.r.t. c_μ and projecting the result onto $\vec{z}$, i.e. by solving

$$\begin{aligned}
\tilde{R^p} &= -\frac{\delta R^p}{\delta c_\mu} z_\mu = -\frac{\partial \tilde{v_j}}{\partial x_j} = 0 \\
\tilde{R_i^v} &= \frac{\delta R_i^v}{\delta c_\mu} z_\mu = \tilde{v_j}\frac{\partial v_i}{\partial x_j} + v_j\frac{\partial \tilde{v_i}}{\partial x_j} - \frac{\partial \tilde{\tau}_{i,j}}{\partial x_j} + \frac{\partial \tilde{p}}{\partial x_i} = 0, \quad i = 1,2 \\
\tilde{R^q} &= \frac{\delta R^q}{\delta c_\mu} z_\mu = -\frac{\partial \tilde{u_j}}{\partial x_j} = 0 \\
\tilde{R_i^u} &= \frac{\delta R^u}{\delta c_\mu} z_\mu = \tilde{u_j}\frac{\partial v_j}{\partial x_i} + u_j\frac{\partial \tilde{v_j}}{\partial x_i} - \tilde{v_j}\frac{\partial u_i}{\partial x_j} - v_j\frac{\partial \tilde{u_i}}{\partial x_j} - \frac{\partial \tilde{\tau}^a_{i,j}}{\partial x_j} + \frac{\partial \tilde{q}}{\partial x_i} = 0, \quad i = 1,2
\end{aligned} \tag{15}$$

Once eqs. 15 are satisfied, the projected $b-c$ mixed derivatives are computed through

$$\begin{aligned}
\frac{\delta^2 F}{\delta c_\mu \delta b_n} z_\mu = \int_\Omega \Bigg(& \tilde{q}\frac{\partial v_j}{\partial x_k} + q\frac{\partial \tilde{v_j}}{\partial x_k} - v_j\tilde{u_i}\frac{\partial v_i}{\partial x_k} - u_i\tilde{v_j}\frac{\partial v_i}{\partial x_k} - u_i v_j\frac{\partial \tilde{v_i}}{\partial x_k} - \tilde{\tau}^a_{ij}\frac{\partial v_i}{\partial x_k} - \tau^a_{ij}\frac{\partial \tilde{v_i}}{\partial x_k} \\
& + \tilde{u_i}\frac{\partial \tau_{ij}}{\partial x_k} + u_i\frac{\partial \tilde{\tau}_{ij}}{\partial x_k} - \tilde{u_j}\frac{\partial p}{\partial x_k} - u_j\frac{\partial \tilde{p}}{\partial x_k}\Bigg)\frac{\partial}{\partial x_j}\left(\frac{\delta x_k}{\delta b_n}\right) d\Omega + \int_{S_w}\left(\tilde{p}\delta_i^j - \tilde{\tau}_{ij}\right) r_i \frac{\delta\left(n_j dS\right)}{\delta b_n}
\end{aligned} \tag{16}$$

The total cost of pFOSM is 4 EFS per cycle, independent from both M and N.

The three groups of derivatives necessary for the final computation of the SD, i.e. $\frac{\delta F}{\delta c_\mu}$, $\frac{\delta F}{\delta b_n}$ and $\frac{\delta^2 F}{\delta c_\mu \delta b_n} z_\mu$ are validated against Finite Differences (FD). Regarding $\frac{\delta F}{\delta a_\infty}$, its value is computed as -0.02919 with FD and -0.02973 using adjoint (1.89% difference). The validation of the other two groups of derivatives is presented in fig. 1.

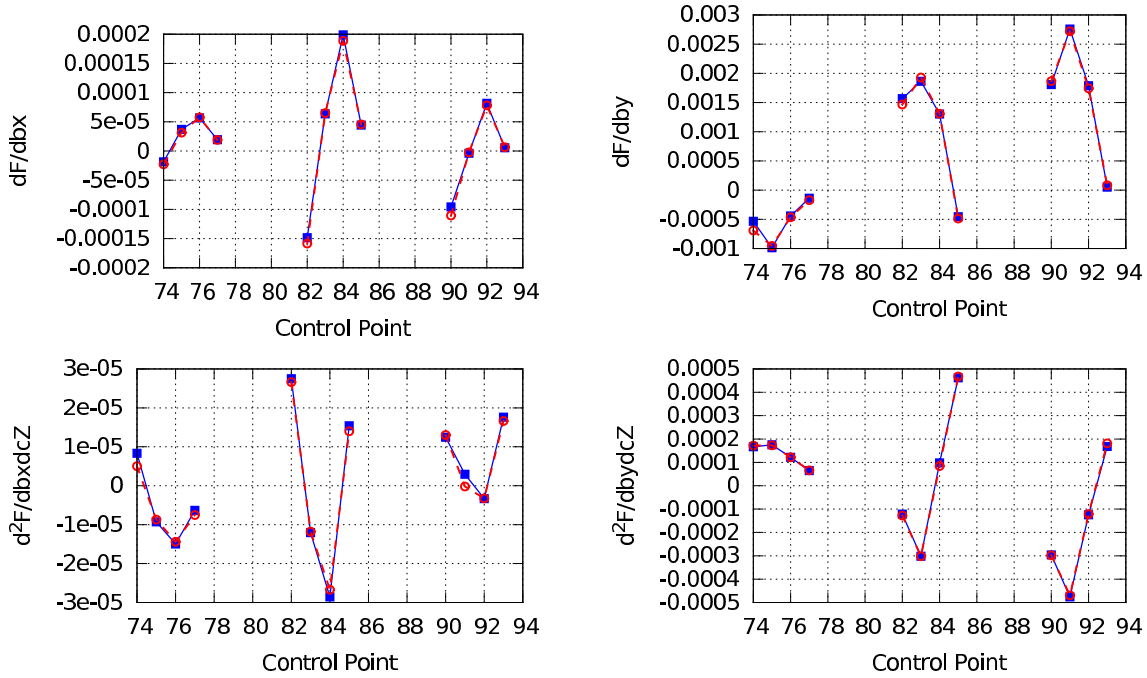

Figure 1: Results obtained with FD (blue filled squares) and the proposed method (red empty circles) for $\frac{dF}{db_n}$ (top) and $\frac{\delta^2 F}{\delta c_\mu \delta b_n} z_\mu$ (bottom).

4.2 Continuous Adjoint to the iPCE

Having formulated and validated the iPCE equations ($M = 1$, $\gamma = 2$), the next step is to compute the gradient of the objective function w.r.t. the design variables ($\frac{dJ}{db_n}$). For this computation, the continuous adjoint method is also used, thus, the new field adjoint equations should be formulated, along with boundary conditions and sensitivity derivatives. The cost of solving the adjoint equations is L EFS; hence, for the optimization loop, the total cost per cycle is $2L$ EFS (6 for $M = 1$, $\gamma = 2$). The augmented objective function is

$$J_{aug} = J + \int_\Omega {}^0R_i^v u_{i0} d\Omega + \int_\Omega {}^0R^p q_0 d\Omega + \int_\Omega {}^1R_i^v u_{i1} d\Omega + \int_\Omega {}^1R^p q_1 d\Omega + \int_\Omega {}^2R_i^v u_{i2} d\Omega + \int_\Omega {}^2R^p q_2 d\Omega \tag{17}$$

where u_{il} and q_l are the adjoint iPCE velocity and pressure fields, respectively. The continuous adjoint development, which is omitted here in the interest of space, yields the field adjoint equations

$$\begin{aligned}
&\frac{\partial u_{il}}{\partial x_i} = 0, \quad l = 0, 1, 2 \\
&u_{j0}\frac{\partial v_{j0}}{\partial x_i} - \frac{\partial (u_{i0}v_{j0})}{\partial x_j} + u_{j1}\frac{\partial v_{j1}}{\partial x_i} - \frac{\partial (u_{i1}v_{j1})}{\partial x_j} + 2u_{j2}\frac{\partial v_{j2}}{\partial x_i} - 2\frac{\partial (u_{i2}v_{j2})}{\partial x_j} + \frac{\partial q_0}{\partial x_i} - \frac{\partial \tau^a_{ij0}}{\partial x_j} = 0 \\
&u_{j1}\frac{\partial v_{j0}}{\partial x_i} - \frac{\partial (u_{i1}v_{j0})}{\partial x_j} + u_{j0}\frac{\partial v_{j1}}{\partial x_i} - \frac{\partial (u_{i0}v_{j1})}{\partial x_j} + 2u_{j1}\frac{\partial v_{j2}}{\partial x_i} - \frac{\partial (u_{i1}v_{j2})}{\partial x_j} + 2u_{j2}\frac{\partial v_{j1}}{\partial x_i} - 2\frac{\partial (u_{i2}v_{j1})}{\partial x_j} \\
&+ \frac{\partial q_1}{\partial x_i} - \frac{\partial \tau^a_{ij1}}{\partial x_j} = 0 \\
&4u_{j2}\frac{\partial v_{j2}}{\partial x_i} - 4\frac{\partial (u_{i2}v_{j2})}{\partial x_j} + u_{j1}\frac{\partial v_{j1}}{\partial x_i} - \frac{\partial (u_{i1}v_{j1})}{\partial x_j} + u_{j0}\frac{\partial v_{j2}}{\partial x_i} - \frac{\partial (u_{i0}v_{j2})}{\partial x_j} + u_{j2}\frac{\partial v_{j0}}{\partial x_i} - \frac{\partial (u_{i2}v_{j0})}{\partial x_j} \\
&+ \frac{\partial q_2}{\partial x_i} - \frac{\partial \tau^a_{ij2}}{\partial x_j} = 0
\end{aligned} \tag{18}$$

where τ^a_{ijk} is the adjoint stress tensor of the k^{th} iPCE field. As far as the boundary conditions are concerned, at the inlet of the domain, zero Dirichlet condition is imposed to u_i and zero Neumann to q_i. Along the parameterized walls zero Neumann to q_i and Dirichlet to u_i equal to $u_0 = -w_0 r_i$, $u_1 = -\frac{w_1 F_1 r_i}{\sqrt{(F_1^2+2F_2^2)}}$, $u_2 = -\frac{2w_1 F_2 r_i}{\sqrt{(F_1^2+2F_2^2)}}$. Finally, for the outlet, Dirichlet boundary condition is imposed to $q_l = u_i^n v_j^n \langle H_i, H_j, H_l\rangle + 2\nu \frac{\partial u_i^n}{\partial n}\langle H_i, H_l\rangle$. For u_l: $v_i^n u_j^t \langle H_i, H_j, H_l\rangle + \nu(\frac{\partial u_i^t}{\partial n} + \frac{\partial u_i^n}{\partial t})\langle H_i, H_l\rangle = 0$, where superscripts n, t stand for the normal and the tangential component of the velocity respectively.

Once eqs. 18 are solved, the SD are computed by

$$\frac{\delta J}{\delta b_n} = \int_{Sw} \left(w_0(-\tau_{ij0} + p_0\delta_i^j) + \frac{w_1 F_1(-\tau_{ij1} + p_1\delta_i^j)}{\sqrt{F_1^2 + 2F_2^2}} + \frac{2w_1 F_2(-\tau_{ij2} + p_2\delta_i^j)}{\sqrt{F_1^2 + 2F_2^2}} \right) r_i \frac{\delta(n_j dS)}{\delta b_n}$$
$$- \int_\Omega \Bigg(u_{i0}v_{j0}\frac{\partial v_{i0}}{\partial x_k} + u_{i0}v_{j1}\frac{\partial v_{i1}}{\partial x_k} + 2u_{i0}v_{j2}\frac{\partial v_{i2}}{\partial x_k} + u_{i1}v_{j1}\frac{\partial v_{i0}}{\partial x_k} + u_{i1}v_{j0}\frac{\partial v_{i1}}{\partial x_k} + 2u_{i1}v_{j2}\frac{\partial v_{i1}}{\partial x_k}$$
$$+ 2u_{i1}v_{j1}\frac{\partial v_{i2}}{\partial x_k} + 8u_{i2}v_{j2}\frac{\partial v_{i2}}{\partial x_k} + 2u_{i2}v_{j1}\frac{\partial v_{i1}}{\partial x_k} + 2u_{i2}v_{j0}\frac{\partial v_{i2}}{\partial x_k} + 2u_{i2}v_{j2}\frac{\partial v_{i0}}{\partial x_k} + u_{j0}\frac{\partial p_0}{x_k}$$
$$+ u_{j1}\frac{\partial p_1}{x_k} + 2u_{j2}\frac{\partial p_2}{x_k} + \tau^a_{ij0}\frac{\partial v_{i0}}{\partial x_k} - u_{i0}\frac{\partial \tau_{ij0}}{\partial x_k} + \tau^a_{ij1}\frac{\partial v_{i1}}{\partial x_k} - u_{i1}\frac{\partial \tau_{ij1}}{\partial x_k} + 2\tau^a_{ij2}\frac{\partial v_{i2}}{\partial x_k}$$
$$- 2u_{i2}\frac{\partial \tau_{ij2}}{\partial x_k} - q_0\frac{v_{j0}}{\partial x_k} - q_1\frac{v_{j1}}{\partial x_k} - 2q_2\frac{v_{j2}}{\partial x_k} \Bigg) \frac{\partial}{\partial x_j}\left(\frac{\delta x_k}{\delta b_n}\right) \tag{19}$$

The SD computed through eq. 19 are validated against FD, fig. 2. Two different sets of weights are used ($w_0 = 1$, $w_1 = 0$ and $w_0 = 0$, $w_1 = 1$), corresponding to μ_F and σ_F and the derivatives of both are in close agreement with FD.

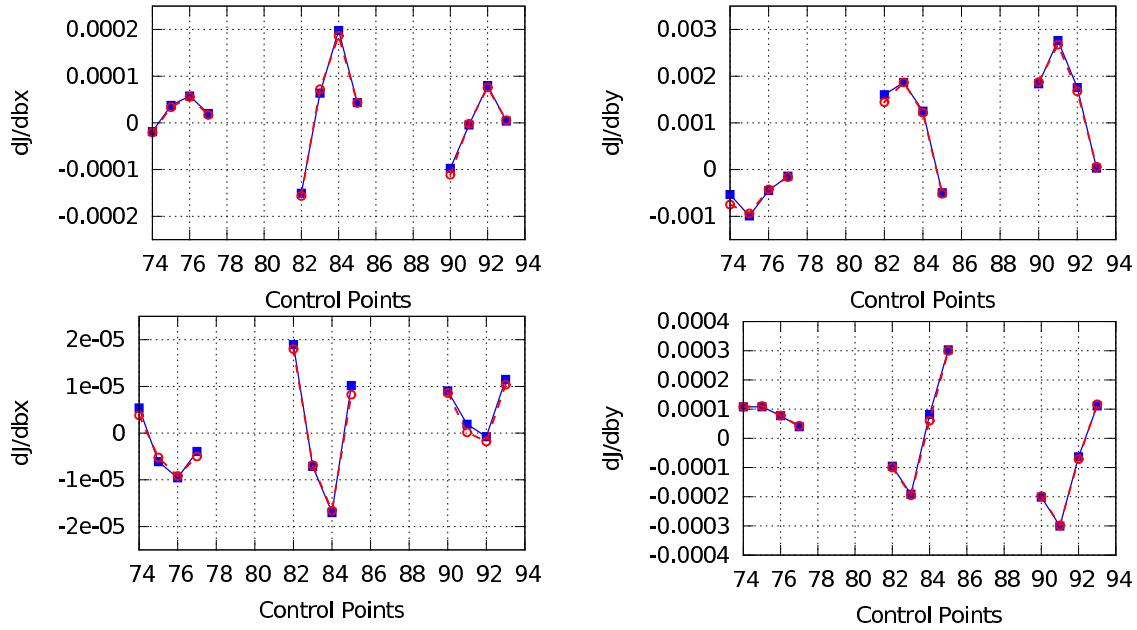

Figure 2: $\frac{dJ}{db_n}$ computed with FD (blue filled squares) and the adjoint iPCE (red empty circles) for $w_0 = 1$, $w_1 = 0$ (top) and $w_0 = 1$, $w_1 = 0$ (bottom).

4.3 Optimization Results

The Volumetric B-Splines control box depicted in fig. 3 was used to parameterize the airfoil. A number of optimization runs was performed in order to form a Pareto front of non-dominated solutions, fig. 4. All optimization runs were conducted under the constraint of constant volume for the airfoil, implemented through the constraint projection method.

Depending on the correlation between the different weight values, more importance was given to either μ_F or σ_F. For the cases with weights (1,6) and (1,7), the final geometry has both μ_F and σ_F improved, which is a very desirable feature. In general, the results of both methods are quite similar and the optimization had a great impact on the σ_F reduction (up to 80% reduction). The initial geometry and the final optimized shapes produced by iPCE and pFOSM for weights (1,0) and (0,1) are presented in fig. 1. The geometrical tendencies between the methods are similar too. Due to volume constraints, displacements are limited, making it impossible to present all geometries in the same figure, however, one should imagine that they are bounded by the green and red geometries.

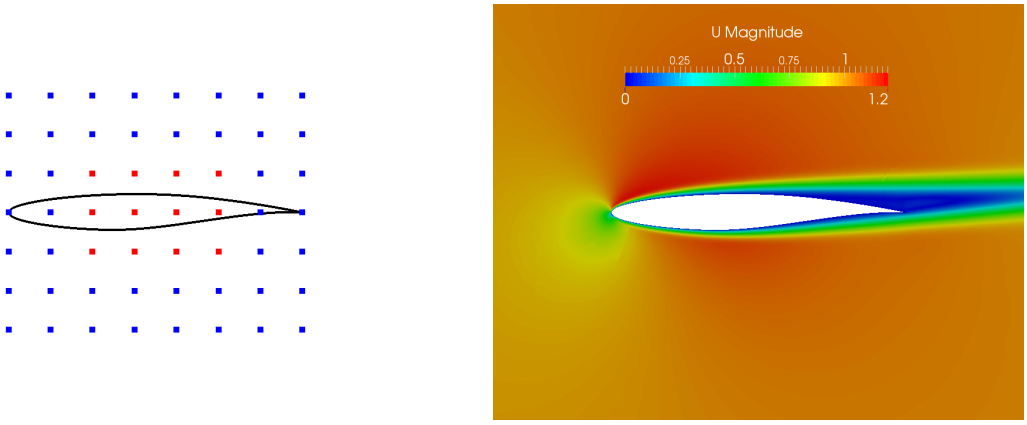

Figure 3: Airfoil shape and control box, with active control points colored in red and inactive in blue (left) and velocity magnitude for $Re = 3000$ and $\alpha_\infty = 4^o$ (right).

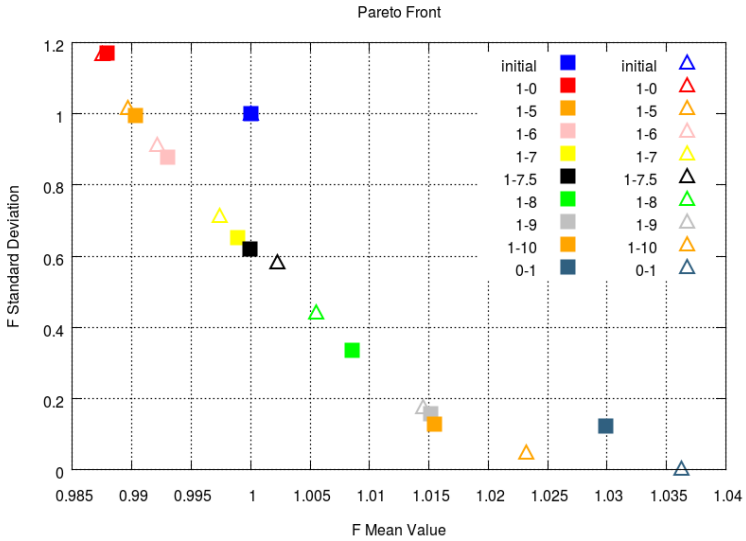

Figure 4: Pareto front for μ_F and σ_F. All values are normalized with the ones corresponding to the initial geometry (filled squares iPCE, empty triangles pFOSM).

Figure 5: Comparison of the initial (red curve), μ_F optimal (blue curve) and σ_F optimal (green curve) geometries designed by pFOSM (left) and iPCE (right).

5 Summary - Conclusions

This paper presents two different methods for quantifying uncertainty in incompressible flows, FOSM and iPCE. For the problem examined, the results concerning UQ were very satisfactory for both methods, even if the former is a first-order one. Both require the development of additional equations and solvers (the adjoint and iPCE ones, respectively), though for the former, the adjoint solver was already available.

Moreover, computational tools for aerodynamic optimization under uncertainties were developed using continuous adjoint to compute the gradients of the FOSM- and iPCE-based UQ metrics and the latter were validated against FD. The adjoint to the iPCE equations and a novel method for computing the projected second-order derivatives (the pFOSM approach), emerging when using FOSM in a gradient-based optimization, were developed for the first time in the literature; the latter led to the developed of a robust design algorithm with a cost that does not scale with either the number of design or the uncertain variables. Applying the developed methods for minimizing the weighted sum of the mean value and standard deviation of the drag force exerted on an airfoil led to a Pareto front of non-dominated solutions; the cost per optimization cycle along with the cost for UQ is presented in table 2. Regarding future work, the extension to turbulent flows for both methods or the development of a second order MoM (SOSM), is foreseen.

Table 2: Computational cost for UQ and optimization with pFOSM and iPCE methods.

	UQ Cost (EFS)	Optimization Cost (EFS)
pFOSM	2	4
iPCE	$\frac{(2+M)!}{2M!}$	$\frac{(2+M)!}{M!}$

REFERENCES

[1] C. Dinescu, S. Smirnov, C. Hirsch, and C. Lacor. Assessment of intrusive and non-intrusive non-deterministic CFD methodologies based on polynomial chaos expansion. *International Journal of Engineering Systems Modeling and Simulations*, 2:87–98, 2010.

[2] K. Kantarakias, M. Chatzimanolakis, V. Asouti, and K. Giannakoglou. On the development of the 3D Euler equations using intrusive PCE for uncertainty quantification. In *2nd ECCOMAS Thematic Conference, UNCECOMP 2017*, Rhodes island, Greece, June 15-17 2017.

[3] I.S Kavvadias, E.M. Papoutsis-Kiachagias, and K.C. Giannakoglou. On the proper treatment of grid sensitivities in continuous adjoint methods for shape optimization. *Journal of Computational Physics*, 301:1–18, 2015.

[4] C. Lacor, C. Dinescu, C. Hirsch, and S. Smirnov. *Implementation of Intrusive Polynomial Chaos in CFD Codes and Application to 3D Navier-Stokes.* Springer International Publishing, 2013.

[5] D. Papadimitriou and K. Giannakoglou. Aerodynamic design using the truncated Newton algorithm and the continuous adjoint approach. *International Journal for Numerical Methods in Fluids*, 68(6):724–739, 2012.

[6] E. Papoutsis-Kiachagias and K. Giannakoglou. Continuous adjoint methods for turbulent flows, applied to shape and topology optimization: Industrial applications. *Archives of Computational Methods in Engineering*, 23(2):255–299, 2016.

[7] E. Papoutsis-Kiachagias, D. Papadimitriou, and K. Giannakoglou. Robust design in aerodynamics using 3rd-Order sensitivity analysis based on discrete adjoint. Application to quasi-1D flows. *International Journal for Numerical Methods in Fluids*, 69(3):691–709, 2012.

[8] D. Xiu and J. Hesthaven. High-order collocation methods for differential equations with random inputs. *SIAM J. Sci. Comput.*, 27:1118–1139, 2005.